Geophysical Journal International

Geophys. J. Int. (2014) doi: 10.1093/gji/ggu155

Geophysical Journal International Advance Access published June 2, 2014

Magnetic parameters and their palaeoclimatic implications—the sediment record of the last 15 500 cal. BP from Laguna Potrok Aike (Argentina)

M.A. Irurzun,[1] M.J. Orgeira,[2] C.S.G. Gogorza,[1] A.M. Sinito,[1] R. Compagnucci[3] and B. Zolitschka[4]

[1] *Instituto de Física Arroyo Seco, IFAS–CIFICEN–CONICET–UNCPBA, Pinto* 399, *Tandil, Buenos Aires, Argentina. E-mail: airurzun@exa.unicen.edu.ar*
[2] *CONICET, Departamento de Ciencias Geológicas, Facultad de Ciencias Exactas y Naturales, Universidad de Buenos Aires, Cd. Universitaria, Pabellón II,* 1428 *Buenos Aires, Argentina*
[3] *CONICET, Departamento de Ciencias de la Atmósfera, Facultad de Ciencias Exactas y Naturales, Universidad de Buenos Aires, Cd. Universitaria, Pabellón II,* 1428 *Buenos Aires, Argentina*
[4] *GEOPOLAR, Institute of Geography, University of Bremen, Celsiusstr. FVG-M, D-*28359 *Bremen, Germany*

Accepted 2014 April 25. Received 2014 March 25; in original form 2013 December 18

SUMMARY

Lake sediments are excellent sources of palaeoenvironmental and palaeoclimatic information because they provide continuous and high-resolution records. South America is of particular interest because it is the only landmass that stretches southward into the Pacific and Atlantic Oceans towards Antarctica. The aim of this study is to explore the relationship of magnetic parameters with elemental and palaeobiological data of Laguna Potrok Aike to develop a model of lake-level changes and related hydrological and climatic fluctuations. Magnetic measurements were performed on subsamples from 15 500 cal. BP to the present, and associated rock magnetic parameters were calculated to infer magnetic mineralogy, concentration and grain size. According to the model, parameters dependent on magnetic concentration and grain size are directly related to lake-level changes. During dry periods, the remanent coercivity displays high values, whereas the proportion of magnetite is relatively low. Low percentages of greigite are observed, indicating that the water of the lake was stratified at least four times during the studied period, at approximately 10 300, 8900, 8500 and 8300 cal. BP. The preservation of greigite by inhibiting its complete transformation into pyrite is associated with a rapid burial that occurs with high sedimentation rates. Thermal stratification could be caused by a slight cooling in the area triggered by a weakening of the Westerlies and/or low activity of the sun, sum to the effect of a flood of melt water in the North Atlantic.

Key words: Magnetic anomalies: modelling and interpretation; Rock and mineral magnetism; South America.

1 INTRODUCTION

To validate global climate models from a magnetic perspective, it is necessary to obtain additional data from the Southern Hemisphere (SH) because such data are scarce compared to the data available for the Northern Hemisphere (NH). On the other hand, lake sediments provide continental records for climate changes and offer higher-resolution than marine sediments (Bradley 1999). Every change in the catchment area of a lake (e.g. changes in rainfall and temperature and differences in sediment erosion and transportation) is reflected in variations of biological, chemical and physical parameters of the responding lacustrine sediment record. Particularly, concentration, composition and/or grain size of magnetic parameters are widely used as proxies for palaeoenvironmental variations (e.g. Stockhausen & Zolitschka 1999; Dearing *et al.* 2001; Hu *et al.* 2002; Paasche *et al.* 2004; Peck *et al.* 2004; Demory *et al.* 2005; Vigliotti *et al.* 2008; Brown & Duguay 2010; Cartwright *et al.* 2011).

Regarding the area studied in this contribution, inferred regional palaeoprecipitation and consequential lake-level fluctuations do not display an overall agreement between the proxies analysed by several authors. The main discrepancies were found for the period between 13 500 and 11 500 cal. BP. Some authors obtained high lake levels and oligotrophic conditions for the Younger Dryas (YD; Massaferro *et al.* 2013) while others found lower lake levels during drier and warmer climate conditions with relatively weak westerlies (Hahn *et al.* 2013; Jouve *et al.* 2013). Zhu *et al.* (2013) and Mayr *et al.* (2013) conclude that a strong wind condition and an increasing

wind-induced wave effect on the lake were produced from 13 000 to 10 970 cal. BP. Zolitschka *et al.* (2013) proposed two options for the elevation of the lake level for the period between 17 000 and 10 500 cal. BP: option 1 represents a decrease in the lake level similar to current levels and option 2 represents a continuously high lake level with a slight decrease from the overflow level to water depths similar to the 'Little Ice Age' (LIA). The main reason for the discrepancies between proxies, primarily during late Pleistocene to early Holocene, is that every proxy variation can be caused by several climate forcings.

A general agreement is found around 17 000 cal. BP and for the beginning of the Holocene, where high lake levels were found (Anselmetti *et al.* 2009; Kliem *et al.* 2013a; Schäbitz *et al.* 2013). A consensus about an evident lake-level decrease was reached with different proxies at approximately the same period, between 9000 and 2500 cal. BP (Hahn *et al.* 2013; Kliem *et al.* 2013a; Massaferro *et al.* 2013; Schäbitz *et al.* 2013). During this time interval, an increase in the lake level and precipitation were suggested by several palaeoshorelines (Anselmetti *et al.* 2009; Massaferro *et al.* 2013). Several proxies indicate a new high lake level during the LIA (e.g. Haberzettl *et al.* 2005, 2007; Kliem *et al.* 2013a; Schäbitz *et al.* 2013; Zolitschka *et al.* 2013). Thereafter, a decreasing water volume until the present day has been suggested by all authors.

The purpose of this study is to present new data of rock magnetic parameters and to explore their relationship with climatic changes compared to other investigations of the same site. In particular, magnetic minerals can be formed under specific circumstances, so the results of these mineral parameters can be used as indicators of specific environmental conditions.

2 SITE DESCRIPTION

Laguna Potrok Aike is a maar lake located in the Patagonian steppe of southern Santa Cruz Province, Argentina (51°57′S, 70°24′W, Fig. 1). The origin of the lake is phreatomagmatic because remnants of a hyaloclastic tephra layer have been detected. Therefore, a maar explosion is assumed (Zolitschka *et al.* 2006). The crater lake is almost circular, with a diameter of c. 3.4 km and a water volume of 0.4 km^3. The potential sediment supply is from a large catchment area (>200 km^2) that extends south into Chile (Coronato *et al.* 2013). The catchment lithology is formed by Pleistocene glacial sediments from the Andean Cordillera and basalts from the local Pali Aike Volcanic Field (Zolitschka *et al.* 2006; Lisé-Pronovost *et al.* 2013). The water depth of the lake is 100 m, and the mean summer temperature is approximately 10–12 °C (Zolitschka *et al.* 2006; Haberzettl *et al.* 2007). The lake is influenced by groundwater

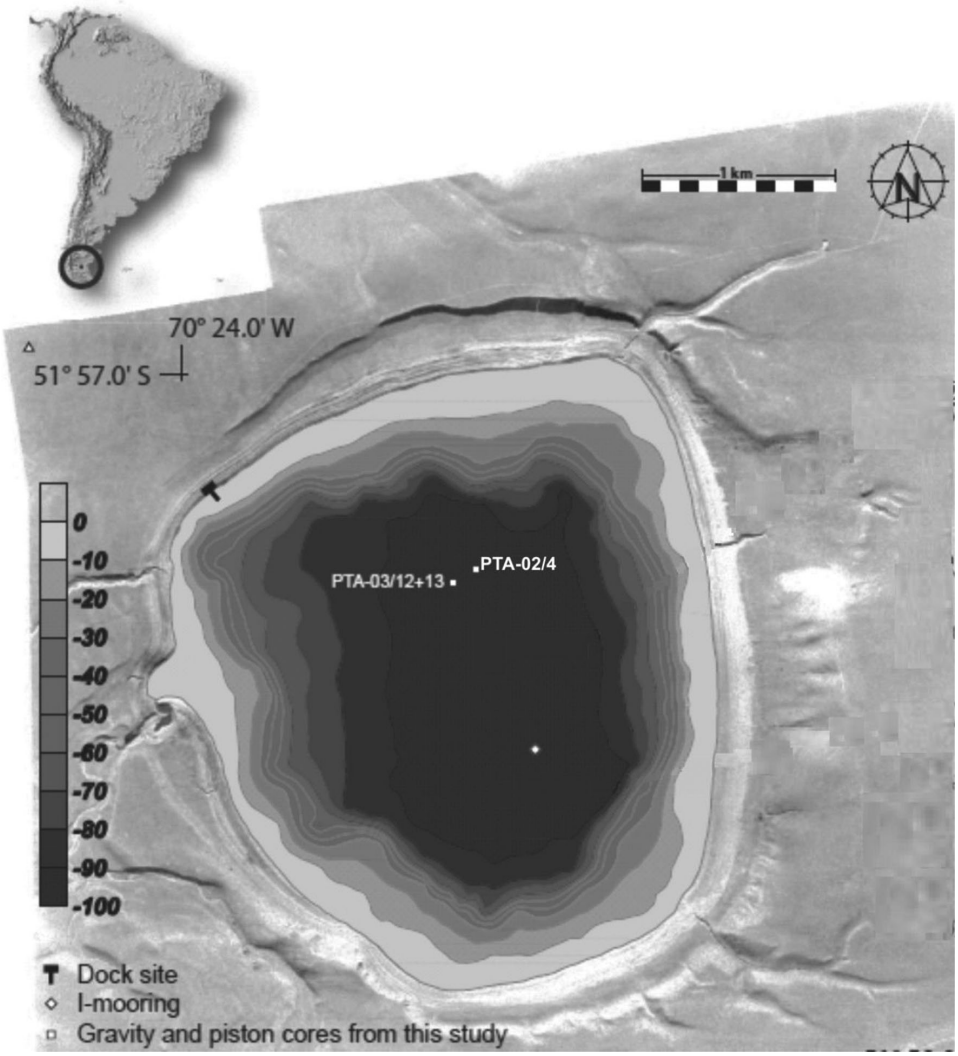

Figure 1. Location map with indicated coring sites of PTA-02/4, PTA-03/12 and PTA-03/13.

variations that allow only minor interannual lake-level variations. Since 1999, these seasonal fluctuations have been in the range of 1–2 m (Ohlendorf *et al.* 2013).

Precipitation decreases from west to east in the Pali Aike Volcanic Field and is less than 300 mm at the site of Laguna Potrok Aike. Surface inflow is only occasional and no longer produces a surface outflow. A former outflow is located at the northwestern shoreline (Haberzettl *et al.* 2007). Inflow is restricted to rain and snow-melt during spring, whereas evaporation is influenced by temperature and wind speed (Ohlendorf *et al.* 2013). The annual evaporation/precipitation (E/P) ratio reaches values of 24 (Haberzettl *et al.* 2005). Given these conditions, a semi-arid climate dominates, and Laguna Potrok Aike responds sensitively to changes in water balance with rising/falling lake levels (Ohlendorf *et al.* 2013; Kliem *et al.* 2013b). The beaches are covered with pebbles, sand and silt. Basaltic rocks were found in the catchment area by Haberzettl *et al.* (2005) and confirmed through magnetic measurements (Gogorza *et al.* 2011, 2012; Lisé-Pronovost *et al.* 2013). Vegetation around the lake is that of a dry Patagonian steppe with *Poaceae*, herbs and shrubs (Oliva *et al.* 2001).

The limited nitrogen supply and subsaline conditions inhibit algal growth, resulting in mesotrophic conditions in the lake (Wille *et al.* 2007; Mayr *et al.* 2009). Present westerly winds in the area are very strong, reaching mean wind speeds of 32 km h^{-1} (Endlicher 1993) and imposing polymictic conditions in the water column, with neither stratification during summer nor freezing in winter (Zolitschka *et al.* 2006). Stratified conditions may have occurred in the past considering that the theoretical mixing of water depths of Laguna Potrok Aike occurs at 52 m (Zolitschka *et al.* 2006).

3 MATERIAL AND METHODS

The studied sediment gravity cores were from the 100-m-deep central basin of Laguna Potrok Aike and were collected during field work in 2002 and 2003 using a 5-m-long coring chamber of a hand-driven UWITEC piston-coring system to extract cores PTA03/12 (1988 cm long) and PTA03/13 (1003 cm long). A modified ETH (Eldgenössische Technische Hochschule)-gravity corer (Kelts *et al.* 1986) was used to obtain core PTA02/4 (90 cm long). This core has a well-preserved water/sediment interface and thus allows the record to be extended to the present day. A walk-core repository for the storage of sediment cores under optimal conditions was used. Coring locations are shown in Fig. 1. The chronology of this sediment record is based on 18 calibrated accelerator mass spectrometry (AMS) ^{14}C ages measured for different materials (stems of aquatic moss, bulk sediment, calcite fraction of the bulk sample, twig of *Berberis* and bone of *Ctenomys* sp.). The chronology was verified using palaeosecular variations of the geomagnetic field (Gogorza *et al.* 2012; Lisé-Pronovost *et al.* 2013). The age-depth model (Fig. 2a) applied here refers to version 4 developed in the framework of the International Continental Scientific Drilling Program (ICDP) project PASADO (Kliem *et al.* 2013b).

For palaeomagnetic studies, the cores were subsampled with 8 cm^3 cubic plastic boxes at 2.5 cm intervals. After subsampling,

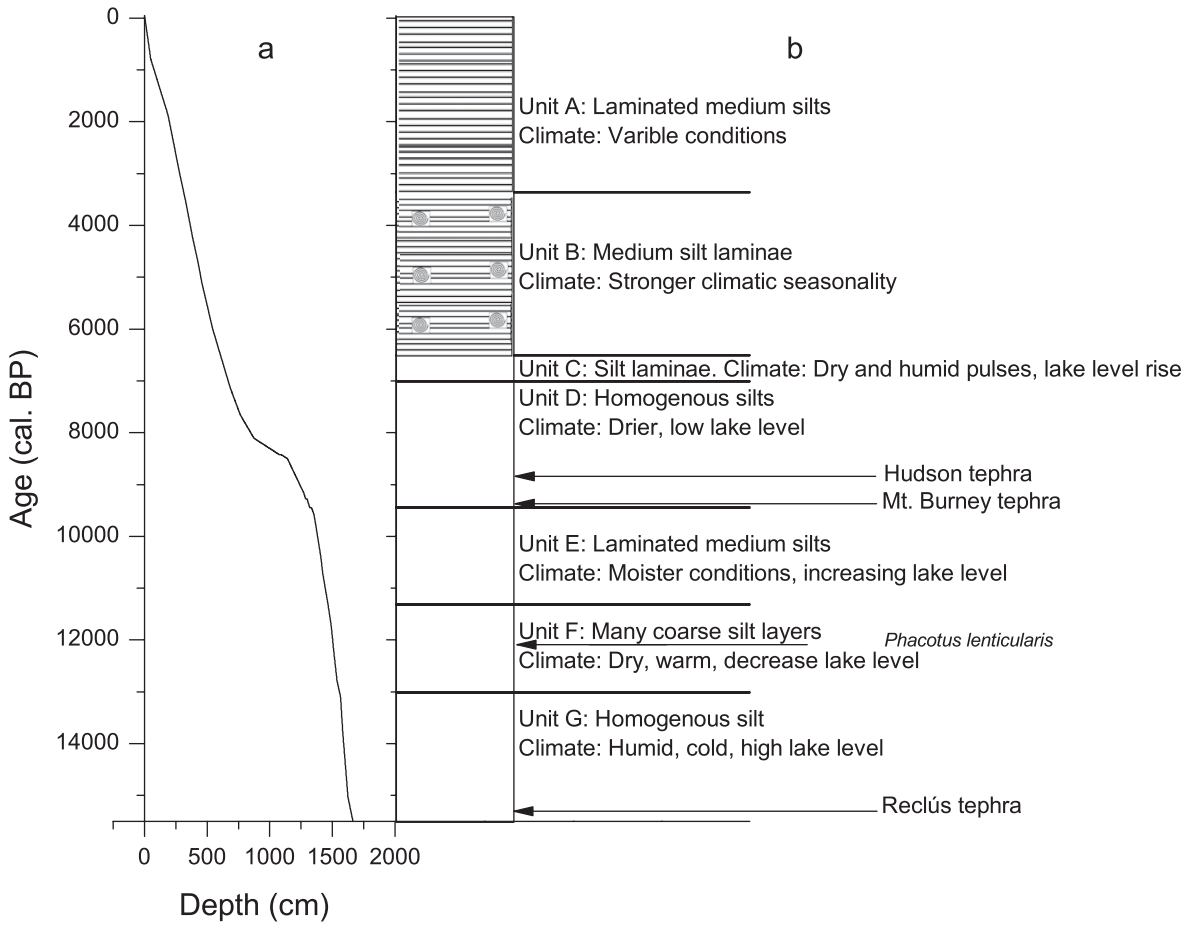

Figure 2. (a) Age-depth model developed by Kliem *et al.* (2013a). (b) Lithological units defined by Haberzettl *et al.* (2007) and some climatic changes from previous studies (Markgraf 1983; Kilian *et al.* 2003; Haberzettl *et al.* 2005; Mancini *et al.* 2005; Haberzettl *et al.* 2007). ◍: Gastropods.

the boxes were sealed and weighed. Several gaps occurred along the profile because the sediment had been used for other investigations. In total, 866 subsamples from the composite record (39 subsamples from PTA02/4, 604 from PTA03/12 and 223 from PTA03/13) were obtained, excluding the tephra layers. Samples were stored at 4 °C until measurements were performed.

Volumetric (κ) and specific (χ) magnetic susceptibility at low and high frequencies (470 and 4700 Hz, respectively) were measured with a Bartington Instruments MS2 system (Carlsbad, CA, USA). An almost continuous composite profile of 1892 cm length (from 2000 to 15 500 cal. BP) was constructed based on a correlation with κ (figs 2 and 3 from Gogorza *et al.* 2012). The composite profile from this work expands from the present to ca. 15 500 cal. BP.

Anhysteretic remanent magnetization (ARM) with an alternating peak field of 100 mT and a steady bias field of 0.05 mT was acquired with a shielded demagnetizer (Molspin Ltd.) and an ARM device. Saturated isothermal remanent magnetization (SIRM) was acquired with a pulse magnetizer (model IM-10–30, ASC Scientific) with a field of 1.2 T and sample exposure to a reversed field in growing steps to obtain remanent coercivity (B_{CR}), soft-IRM (IRM_{-40mT}/SIRM) and the S-ratio (-IRM_{-300mT}/SIRM). Interparametric ratios (ARM/κ, SIRM/κ and ARM/SIRM) were calculated using these results. All remanent magnetizations were measured with a JR6A Dual Speed Spinner Magnetometer (Agico Instruments, Brno, Czech Republic). Hysteresis measurements were made on a select group of samples with a MicroMag 3900 VSM (Princeton Measurements Corporation™, Westerville, OH, USA).

4 LITHOLOGY OF THE STUDIED SEDIMENT CORES

The investigated record consists of clayey and sandy silts that become coarser with depth. There are three tephra layers and reworked sediment sections related to mass-movement deposits, with the latter found especially in the lower half of the core. Haberzettl *et al.* (2007) divided the record into seven units (G to A in Fig. 2b).

The first section, from 1892 to 1557 cm (unit G), consists of dark-brown homogenous silts with plant fragments and a volcanic ash layer. The minerogenic input is explained as a response to a high lake level that resulted in an outflow 25 m above the modern lake level, based on dated lake-level terraces (Zolitschka *et al.* 2013).

The second section covers 1556 to 1465 cm (unit F) and is composed of brown medium silts with many coarse silt layers. This section is the only unit with algal remains of *Phacotus lenticularis,* indicating warmer conditions. A lower lake level as the result of increased evaporation is suggested for this period.

The third section, from 1464 to 1320 cm (unit E), contains dark- and light-brown laminated medium silts with gastropods. Moister conditions are suggested by all geochemical proxies and also by a regional study of grass cuticles from the Patagonia (Markgraf 1983). This higher lake level was caused by increased rainfall and runoff.

The fourth section, from 1319 to 669 cm (unit D), is composed of dark-grey homogenous medium to coarse silts with sandy layers interbedded with gastropods and contains volcanic ashes associated with Mt. Burney (Kilian *et al.* 2003) and Hudson eruptions. Geochemical data suggest that this section represents the lowest lake level for the last 15 500 cal. BP, with two short transgressions (Haberzettl *et al.* 2007). The low lake level interpreted for this sediment section can be explained by the hypothesis suggested by Mancini *et al.* (2005), who inferred higher temperatures and aridity for southern South America during the mid-Holocene.

The fifth section, from 668 to 607 cm (unit C), is composed of thick dark-grey and fine to medium silt laminae with scattered gastropods in the uppermost part. This period is interpreted as dry but with short, humid pulses.

The sixth section, from 606 to 313 cm (unit B), is composed of grey medium silt laminae with a few gastropods. The geochemical lake-level indicators display higher climatic variability with wet and dry conditions.

The seventh section, from 312 cm to the sediment surface (unit A), is composed of laminated medium silts of varying thickness in different shades of brown. Gastropods are absent. Dry conditions are still present with evidence of several humid periods. The last pronounced wet episode is contemporary with the LIA (Haberzettl *et al.* 2005).

5 SIMPLIFIED ENVIRONMENTAL MODEL FOR THE INTERPRETATION OF MAGNETIC PARAMETERS

According to Geiss *et al.* (2003), rock magnetic parameters, analogously to other sediment parameters, are not palaeoclimate proxies *per se* but should be interpreted in terms of climate by establishing a model that links rock magnetic variations to climatic change. In a second step, these magnetic interpretations are related to other proxies. Concentration variations, magnetic grain-size ratios and magnetic mineralogy changes must be analysed simultaneously to develop a model that infers environmental changes using magnetic parameters. Certain assumptions can be made for lakes with lake-level variations that are sensitive to changes in the E/P ratio, such as Laguna Potrok Aike (Vázquez *et al.* 2010; Vázquez 2012). If there is a year-round lack of stratification in the water column, then the particle size only varies in response to (1) lake-level fluctuations causing more or less littoral erosion, (2) variations in runoff and/or (3) changes in wind strength.

Ideally, magnetic grains are of allochthonous origin. This assumption is correct for the minerogenic sediments of Laguna Potrok Aike (Haberzettl *et al.* 2007). Thus, a high concentration of magnetic particles indicates higher minerogenic influx to the lake, that is, more runoff. Considering that grain sizes in lake basins decrease from littoral to profundal zones (Nichols 2009), high concentrations of small magnetic grains are expected for the central part of the lake when the lake level rises. Conversely, a decreasing lake level produces increased grain sizes as the lake shore moves closer to the profundal basin. Therefore, low concentration and larger magnetic grain sizes should be found in sediment cores under low lake-level conditions.

Any change in magnetic mineralogy of the sediment sequence implies changes in the terrigenous input. However, the formation of diagenetic minerals plays an important role and should be studied more carefully to determine when and where the magnetic mineralogy changes occur in the lacustrine environment.

Magnetic parameters and their relations fall into three general categories: magnetic concentration parameters, changes in magnetic grain size and interparametric ratios and changes in magnetic mineralogy

(1) Magnetic concentration parameters χ, SIRM and ARM are sensitive to changes in the concentration of magnetic minerals (e.g. Anderson & Rippey 1988; Lanci *et al.* 1999; Hilgenfeldt 2000; Geiss *et al.* 2003; Rühland *et al.* 2009). χ has high values for superparamagnetic (SP) particles and relatively high values for multidomain (MD) grains (Thompson & Oldfield 1986). ARM is more

sensitive than SIRM to single domain (SD) grains (Turner 1997). The total χ of a sample is the sum of the ferromagnetic, paramagnetic and diamagnetic contributions, whereas SIRM and ARM are independent of paramagnetic minerals. Therefore, all three parameters should be studied simultaneously to infer changes in magnetic concentration.

(2) Changes in magnetic grain size and the interparametric ratios of ARM/κ, ARM/SIRM and SIRM/κ can be used for these interpretations. Low ratios indicate coarse grain sizes, whereas high values suggest fine magnetic grain sizes. The ARM/SIRM ratio is the best estimator of changes in magnetic grain size because neither of the two parameters depends on paramagnetic minerals (Turner 1997). The SIRM/k ratio has high values when greigite is present (Peters & Dekkers 2003; Blanchet *et al.* 2007; Roberts *et al.* 2011). Hysteresis ratios provide additional information about magnetic domains and grain size, assuming that the number of domains increases with grain size (Dunlop 2002).

(3) Changes in magnetic mineralogy can be determined by using the remanent coercive field of SIRM (B_{CR}) or IRM_{-40mT}/SIRM (soft-IRM). High or low B_{CR} indicates hard (hematite, greigite) or soft (magnetite, Ti-magnetite) magnetic minerals, respectively. Soft-IRM behaves in reverse of B_{CR}. Curie temperatures are also good estimators of magnetic mineralogy (Dankers 1978) and suggest the proportion of different constituents in a sample (Irurzun *et al.* 2009).

6 RESULTS

The different χ logs display a strong correlation (Fig. 3a), which enables the three cores to be combined into one composite record (Fig. 4a) to obtain an almost continuous time-series for the last 15 500 cal. BP. Based on this strong correlation, only the composite record will be discussed henceforth.

The main magnetic carrier is pseudo-single domain (PSD) (Ti)-magnetite (Gogorza *et al.* 2012) and does not display significant changes in the record (mean value of S-ratio is 0.969 ± 0.001, Fig. 6). According to Thompson & Oldfield (1986), if the κ versus SIRM (log-log) plot behaves linearly, then the main change in the sample's magnetic parameters is due to differences in the concentration of magnetite (Supporting Information Fig. S2). The scattering observed in the plot could be a result of differences in magnetic grain size (4–16 μm) or the presence of paramagnetic minerals (Gogorza *et al.* 2012).

A typical hysteresis loop found in soft magnetic minerals, such as magnetite with SD or PSD grains (Dunlop & Özdemir 1997), is shown in Supporting Information Fig. S1a. Ninety-five per cent of the samples display this behaviour, and only 5 per cent of the studied samples display a different and unusual behaviour (Supporting Information Fig. S1b). In this case, the hysteresis loop exhibits a wide centre, suggesting the presence of hard magnetic minerals, such as greigite (cf. Roberts *et al.* 2011), and/or a mix of soft and hard magnetic minerals (Tauxe *et al.* 1996). As shown in Supporting Information Fig. S1a, the corrected hysteresis loops indicate saturation fields well below 300 mT, which is a typical coercivity for magnetite according to Richter *et al.* (2006). Supporting Information Fig. S1c presents the relationship among the hysteresis parameter ratios H_{CR}/H_C versus M_{RS}/M_S (Dunlop 2002). The results are in the PSD region for (Ti)-magnetite. Only one sample is in the mixed SD-MD region. The slight difference between the hysteresis curves (corrected/uncorrected) is caused by low

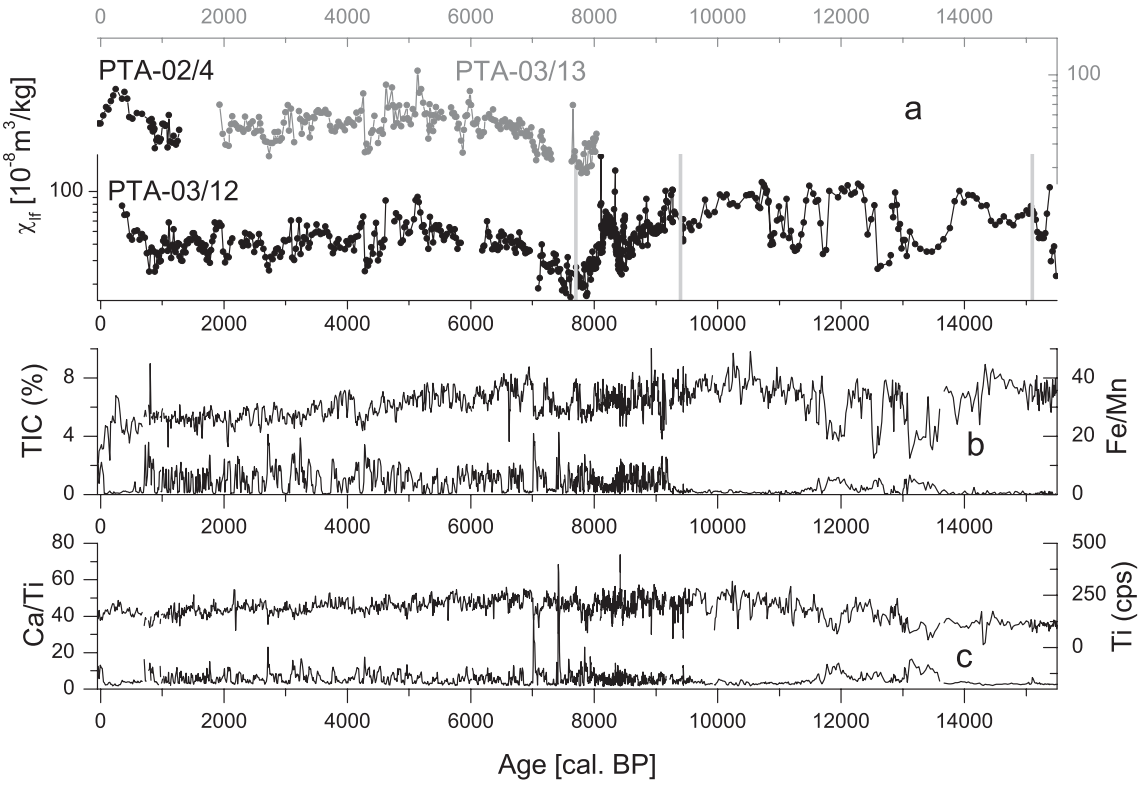

Figure 3. (a) Logs of χ from the two piston cores (PTA-03/12+13) and from the gravity core (PTA-02/4) after correlation versus calibrated age. Hereafter, all the cores will be plotted together. Grey lines indicate prominent tephra layers. (b) Percentages of TIC (black) and Fe/Mn ratio (grey) used by Haberzettl *et al.* (2007) to infer lake-level variations and changes in redox conditions, respectively. (c) Ca/Ti ratio (black) and Ti counts per second (grey) used by Haberzettl *et al.* (2007) to infer lake-level variations and minerogenic input, respectively.

percentages of paramagnetic particles (Supporting Information Figs S1a and S1b). The estimated paramagnetic contributions (per cent paramagnetic $= 100 \times \chi_{\text{low field}}/\chi_{\text{high field}}$, Orgeira *et al.* 2003) have mean values of 7 per cent; this low percentage does not vary considerably along the core, indicating that the observed dispersion in the κ versus SIRM (log-log) plot (fig. 3c from Gogorza *et al.* 2012) is a result of differences in magnetic grain size.

7 APPLICATION OF THE MODEL

Magnetic concentration (Fig. 4) displays the highest variation, followed by magnetic grain size (Fig. 5) and mineralogy (Fig. 6). Therefore, magnetic concentration was used to divide the record into four rock magnetic zones to support our interpretation. Listed from oldest to youngest, these zones are as follows: zone IV (15 500–9400 cal. BP), zone III (9400–7900 cal. BP), zone II (7900–1100 cal. BP) and zone I (1100 cal. BP-present day). Table 1 displays the behaviour of the magnetic parameters used in this study and their palaeoclimatic interpretations.

7.1 Zone IV

Except for two short periods, the mineralogy in zone IV remains constant, with values in the range of magnetite, such as B_{CR} values varying between 30 and 40 mT, SIRM/k between 8 and 12 kA m^{-1} (Peters & Dekkers 2003) and positive values of soft-IRM (Fig. 6a). A different mineralogy is observed approximately at 15 100 and 10 320 cal. BP.

For the sample at 15 100 cal. BP, concentration parameters are on the order of the mean values obtained for zone IV. Fine grain size is suggested, which is consistent with small grains of magnetite (B_{CR} 40.5 mT) in the stable SD range (Thompson & Oldfield 1986). Low values of soft-IRM are observed because IRM measurements are not very sensitive to fine particles. Following the interpretation of Peters and Dekkers (2003), this sample is in the (Ti)-magnetite range (Table 1).

For the sample at 10 320 cal. BP, χ is in the range of the mean values obtained for the zone, but ARM and SIRM have higher values. ARM/k displays a high value but not as high as the value for SIRM/k. Thermal demagnetization was performed to investigate the magnetic components (Fig. 7a). The main magnetic phase lost 81 per cent of SIRM at a Curie temperature (T_C) of 325 °C. The T_C values of greigite and Ti-magnetite are in the range 250–350 °C (Dekkers *et al.* 2000) and 200–350 °C (Dankers 1978), respectively. The secondary phase lost the remainder of its SIRM at 586 °C (the T_C for magnetite is 580 °C, Dankers 1978). According to the main T_C, high B_{CR}, low soft-IRM and high SIRM/k, the main carrier of magnetization in this sample is greigite (Ariztegui & Dobson 1996; Peters & Dekkers 2003; Blanchet *et al.* 2007).

As stated in Section 4, the sediment came from allochthonous sources, and zone IV has the same main magnetic mineralogy. Since the general assumptions are assured, the environmental model is applied except for the sector of the sample at 10 320 cal. BP. χ, SIRM and ARM behave similarly: in general, high values for ARM are most noticeable from 15 300 to 13 800 cal. BP, 12 500 to 11 400 cal. BP and 10 800 to 9700 cal. BP (Fig. 4a), and low values are observed from the bottom of the core to 15 300 cal. BP, 13 800 to 12 500 cal. BP and 11 400 to 10 800 cal. BP. The highest dispersion is obtained in this zone, although SIRM displays smooth changes.

From 15 300 to 13 800 cal. BP, 12 500 to 11 400 cal. BP and 10 800 to 9700 cal. BP, magnetic grain size ratios (Fig. 5a) indicate finer particles and thus a high lake level. Centred at 13 300 cal. BP, the magnetic parameters (Figs 4–6) indicate a noticeable decrease (Table 1) in the lake level.

7.2 Zone III

Zone III displays averaged concentration parameters that are comparable to the remainder of the record, although samples with the highest variability for different parameters are also observed in the rock magnetic zone. B_{CR} and soft-IRM display abrupt changes, suggesting noticeable changes in magnetic mineralogy, primarily in the 9000–8300 cal. BP section (Fig. 6b), which exhibits high B_{CR} and low soft-IRM values (Fig. 6a). Peaks in the concentration are also observed (Fig. 4a) and are distributed periodically (Fig. 4b). However, the magnetic grain size is almost uniform (Fig. 5a). Nevertheless, three samples (located between 8300 and 9000 cal. BP, Fig. 5b) display very high SIRM/k ratios and are in the greigite region (Fig. 7d). Similar to the samples in zone IV, thermal demagnetization of SIRM was applied for one of these samples (Fig. 7b). In the first and predominant phase, 88 per cent of the SIRM is lost at a T_C of 307 °C, which is in the range of greigite or Ti-magnetite. The second phase has a T_C of 578 °C and is near the T_C of magnetite. For those samples, the SIRM/k ratio displays values of 27, 21 and 22 kA m^{-1}, which is considerably higher than the ratios of the remainder of the core; the samples also display high values of $B_{CR,}$ demonstrating that the magnetic carrier is greigite (Peters & Dekkers 2003; Blanchet *et al.* 2007). The presence of greigite is further discussed in Section 8.2.

7.3 Zone II

The B_{CR} values for zone II are approximately 39 mT, and 99 per cent of the samples display a positive soft-IRM, suggesting a homogeneous magnetic mineralogy with magnetite as the main carrier. A group of samples at 7600 and between 5300 and 5100 cal. BP exhibit high B_{CR} and negative values for soft-IRM.

All of the samples in zone II behave similarly as those in zone III; thus, thermal demagnetization was applied (Fig. 7c). The T_C values are 352 °C (74 per cent of SIRM is lost at this temperature) and 589 °C. The magnetic grain size indicators, including SIRM/k, display relatively low values and the B_{CR} values are approximately 50.5, 42 and 43.3 mT, which are consistent with the value for Ti-magnetite (Peters & Dekkers 2003). In these cases, the suggested change in mineralogy is likely related to a higher proportion of Ti in the Ti-magnetite samples compared with the remainder of the core. Certain samples exhibit SIRM/k to ARM/k ratios in the greigite region (Fig. 7d), but the remaining magnetic parameters do not suggest the presence of greigite. Except for the greigite samples, the environmental model can be applied to zone II. Magnetic concentration and grain size parameters exhibit minor variations around the mean value. ARM displays a gradual increase since 7000 cal. BP, likely due to the presence of finer particles; this trend corresponds with the trend suggested by the baseline magnetic grain size indicators (Fig. 5a). Variations in the magnetic grain size are observed at 7420, 5780, 4750 and 2820 cal. BP, indicating lake-level fluctuations superimposed on a long-term increasing trend.

7.4 Zone I

B_{CR} values between 30 and 40 mT and positive values for soft-IRM indicate the presence of (Ti)-magnetite as the carrier of

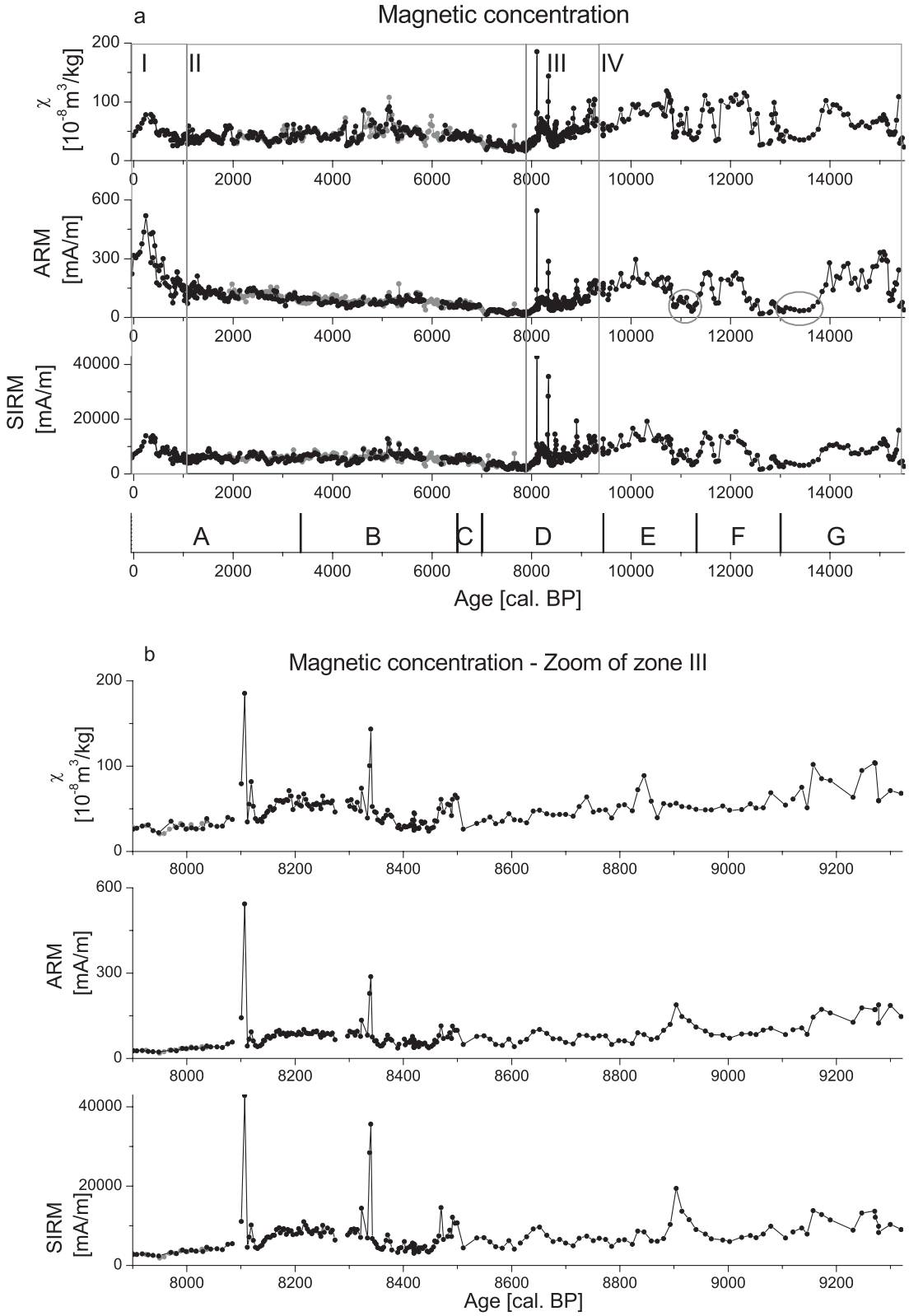

Figure 4. (a) Variation of magnetic concentration for the last 15 500 cal. BP. The lower panel provides the sediment units defined by Haberzettl *et al.* (2007), the upper panel the rock magnetic zones. The circles indicate low lake levels (see Section 7.1). (b) Variations in magnetic concentration for zone III.

magnetization in this zone. The concentration parameters display an increasing trend from 1100 cal. BP until a maximum at 250 cal. BP and a decreasing trend to the present (Fig. 4a). The lowest concentration was observed at approximately 790 cal. BP, which is most noticeable in ARM. ARM/k and ARM/SIRM display the highest values from 1100 to 860 cal. BP and from 550 cal. BP to the top of the record, indicating fine magnetic grain sizes (Fig. 5a). SIRM/k exhibits a similar behaviour, but the trend from 250 cal. BP

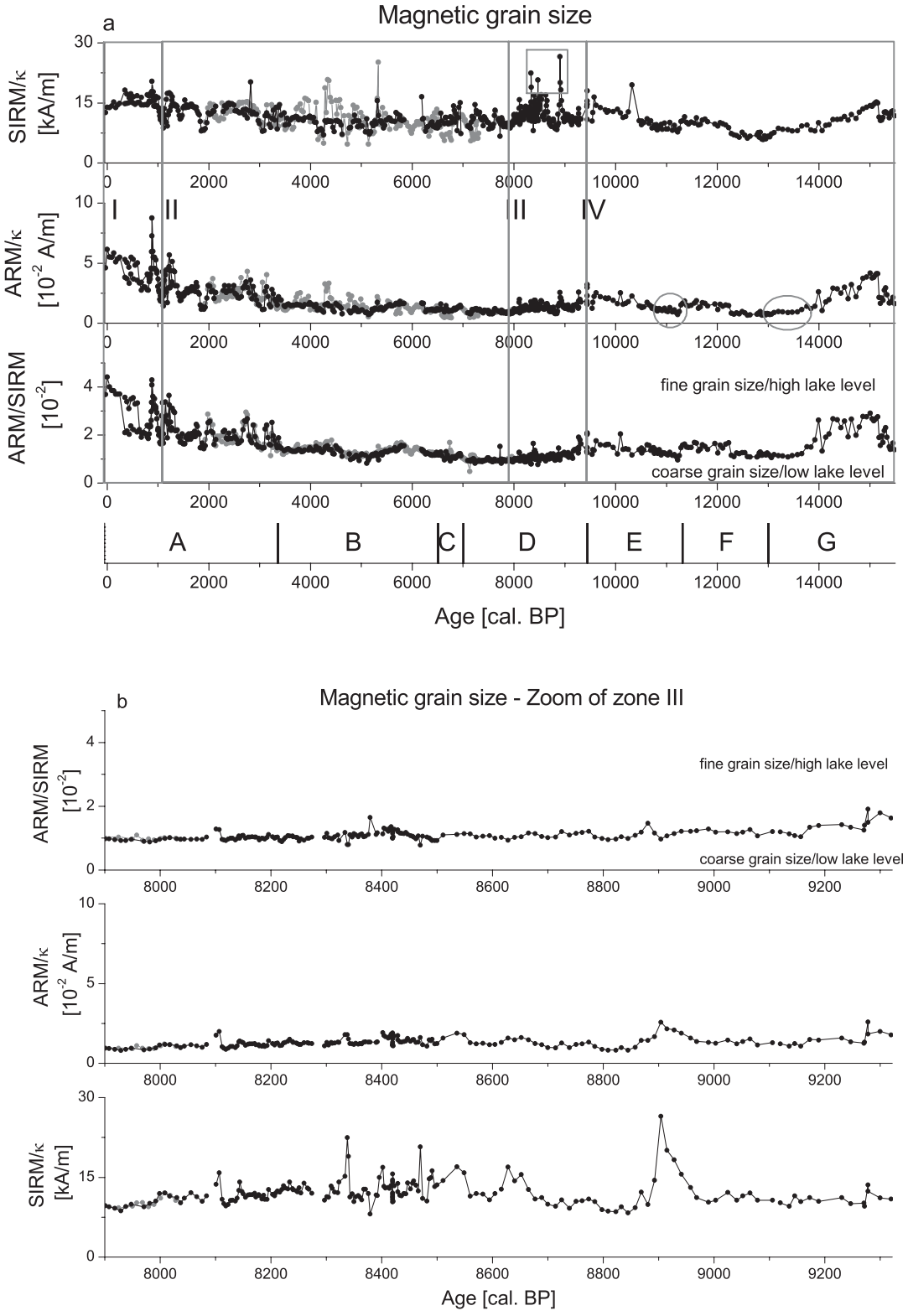

Figure 5. (a) Variation in magnetic grain size for the last 15 500 cal. BP. The lower panel are the regions from defined by Haberzettl *et al.* (2007), the upper panels are zones defined in this work. The circles indicate low lake levels (see Section 7.1) and the square point out the zone with noticeable changes in magnetic parameters (see Section 7.2). (b) Variation in magnetic grain size for the zone III.

to the present is constant. As indicated by the model, an increase in the lake level is suggested at the beginning of the zone. Between 830 and 700 cal. BP, a small decrease in the lake level is suggested, followed by a second increase until 210 cal. BP.

A sample at 210 cal. BP has the finest magnetic grain size of the record (black star in Supporting Information Fig. S1c). Therefore, the different trends of SIRM/k and ARM/k could be because SIRM is less sensitive to smaller particles than ARM. The magnetic

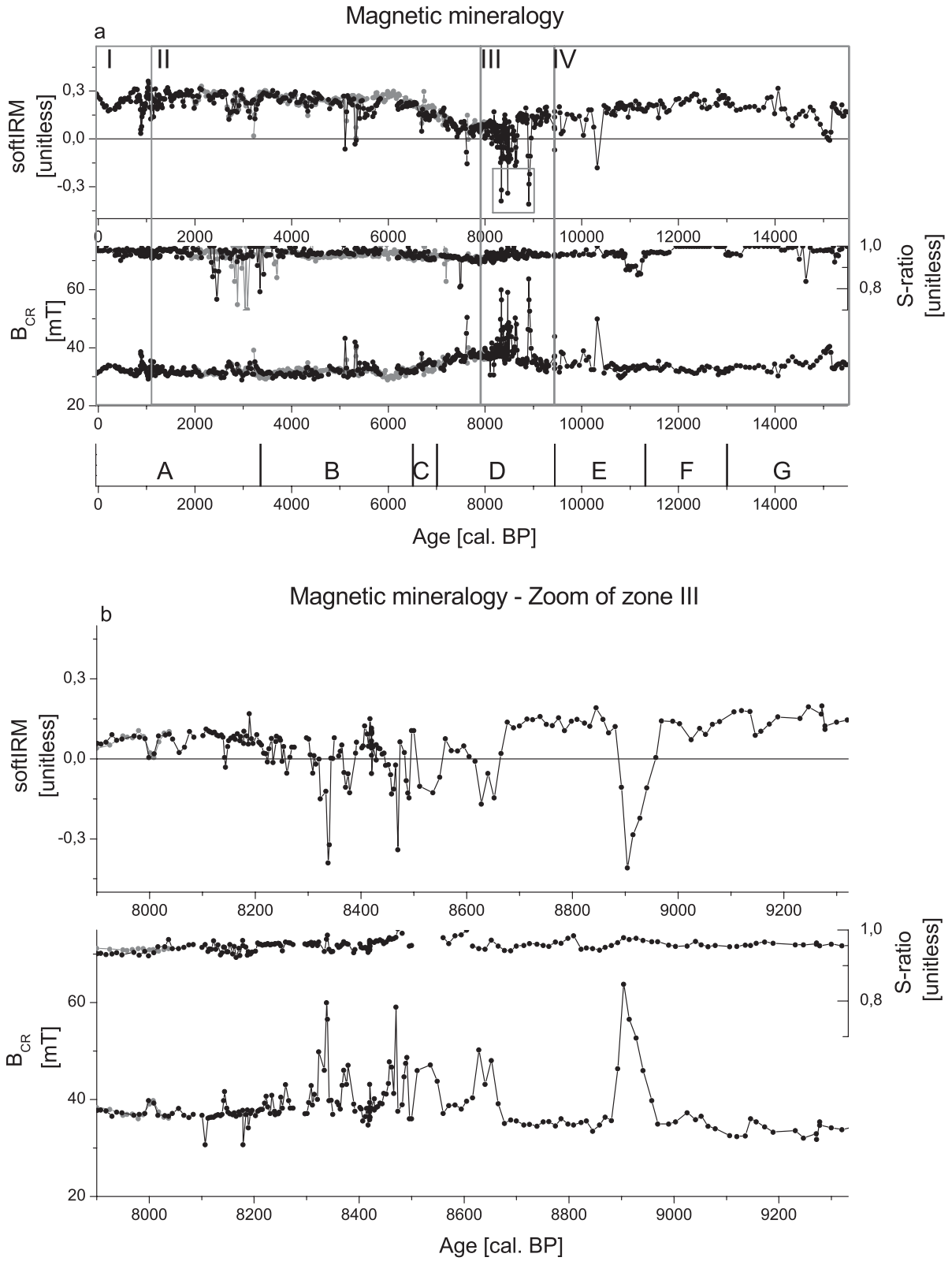

Figure 6. (a) Variation in magnetic mineralogy parameters for the last 15 500 cal. BP. The lower panel are the regions from defined by Haberzettl *et al.* (2007), the upper panels are zones defined in this work. The square point out the zone with noticeable changes in magnetic parameters (see Section 7.2). (b) Variation in magnetic mineralogy parameters for the zone III.

Table 1. Summary of general magnetic characteristics for rock magnetic zones I to IV.

Zone		General description
I	Magnetic concentration	Intermediate to high
	Magnetic grain size	High
	Magnetic mineralogy	(Ti) magnetite
	Lake-level interpretation	High (a slight low in lake level at around 800 cal. BP)
	Environmental conditions	Moister periods also found in other regional records
II	Magnetic concentration	Intermediate(increasing trend in ARM)
	Magnetic grain size	Intermediate(increasing trend)
	Magnetic mineralogy	(Ti) magnetite (some samples with high Ti)
	Lake-level interpretation	Slight variations superimposed to an increasing trend
	Environmental conditions	Moist periods at around 7420; 5780; 4750; 2820 cal. BP
III	Magnetic concentration	Intermediate with some peaks
	Magnetic grain size	Coarse with slight changes
	Magnetic mineralogy	(Ti) magnetite in low proportion (three samples of greigite at 8900; 8500 and 8300 cal. BP)
	Lake-level interpretation	Decrease
	Environmental conditions	Dry conditions
IV	Magnetic concentration	High
	Magnetic grain size	Intermediate (decrease from 10 800 to 9700 cal. BP)
	Magnetic mineralogy	(Ti) magnetite (one samples of greigite at 10 320 cal. BP)
	Lake-level interpretation	High (relatively lower from 13 800 to 10 800 cal. BP)
	Environmental conditions	Higher temperatures during warmer conditions

proxies indicate that the upper-most sample has a lower magnetic concentration and coarser magnetic particles, which indicate a lower lake level.

8 DISCUSSION

8.1 General trends and comparison with previous studies

Zolitschka *et al.* (2013) proposed a curve for lake-level variations using the results from several proxies from different authors. The lake-level variations proposed by Zolitschka *et al.* (2013) were used as a reference line to reconstruct the lake-level changes in this work. A detailed variation to this reference line was added using the environmental model based on magnetic parameters (Fig. 8). The final changes are tested against other regional proxy data.

Zone IV: The high lake level suggested by magnetic parameters between 15 300 and 13 800 cal. BP is consistent with the Laguna Potrok Aike lake level suggested by previous authors (Wille *et al.* 2007; Kliem *et al.* 2013a; Massaferro *et al.* 2013; Zolitschka *et al.* 2013).

The lake level was relatively low from 13 800 to 10 800 cal. BP, possibly due to the higher temperatures and associated elevations of evaporation rates during the warmer conditions of the Late Glacial (Jouve *et al.* 2013). A slight increase in the lake level occurred between 12 500 and 11 400 cal. BP during a warm interval (Fig. 8). This finding could be attributed to a slow retreat of the glaciers during the Late Glacial period that resulted in a decrease in the magnetic grain size (Frank *et al.* 2002). A decrease in the magnetic grain size from 10 800 to 9700 cal. BP could suggest an increase in the lake level. The magnetic results could indicate a middle option between options 1 and 2 suggested by Zolitschka *et al.* (2013), but the trend in magnetic grain size appears to confirm lake-level option 2 with two small decreases.

Zone III: The magnetic parameters indicate an increase in the magnetic grain size between 9500 and 7900 cal. BP (Table 1), which is consistent with a trend towards dry conditions that caused a decrease in the lake level (Zolitschka *et al.* 2013). This finding is also indicated by other proxies, such as diatom and pollen records (Mancini *et al.* 2005; Massaferro *et al.* 2013). Changes in vegetation of the Patagonian Steppe also suggest low lake levels (Wille *et al.* 2007). A low lake level was also assumed for this period using seismic stratigraphy by Anselmetti *et al.* (2009). In addition, a general recession is suggested by high sedimentation rates (Kliem *et al.* 2013a) and the absence of *P. lenticularis* (Jouve *et al.* 2013).

According to geological and geochemical information (Figs 3b and c) and the chronology (Kliem *et al.* 2013a), allochthonous input of detrital material increases in this zone, suggesting that the magnetic signal originates primarily from the littoral zone of the lake. Mineralogical variations and peaks in the concentration of magnetic minerals (Fig. 4a) associated with a slight decrease of particle size (Fig. 5a) were detected. These peaks can be correlated with short transgressive events, as proposed by Haberzettl *et al.* (2007). The presence of greigite is related to authigenesis in the lake during these periods.

Zone II: Slight variations in the lake level between 7400 and 7000 cal. BP (Fig. 8) are detected using magnetic proxies and conclude the extremely dry times. Following our model assumptions, the lake level rises continuously during the remainder of the period (7 000–1100 cal. BP), with rises at 5780, 4750 and 2820 cal. BP (Fig. 8). The existence of shorelines mapped to the seismic data by Anselmetti *et al.* (2009) confirms this trend. The other increase in the lake level from 5400 to 4400 cal. BP is confirmed by a transgression at approximately 4800 cal. BP (Haberzettl *et al.* 2007; Anselmetti *et al.* 2009). Several moist periods were also obtained using geochemical data, which confirm the behaviour of our record between 3800 and 1100 cal. BP (Hahn *et al.* 2013).

Zone I: The application of the model indicates an increase in lake level during two periods between 1100 and 860 cal. BP and between 700 cal. BP and the present. A lower lake level was observed between 860 and 700 cal. BP (Fig. 8). These changes are consistent with the moister periods found through multiproxy analysis by Haberzettl *et al.* (2005). Other regional records, such as from Lago

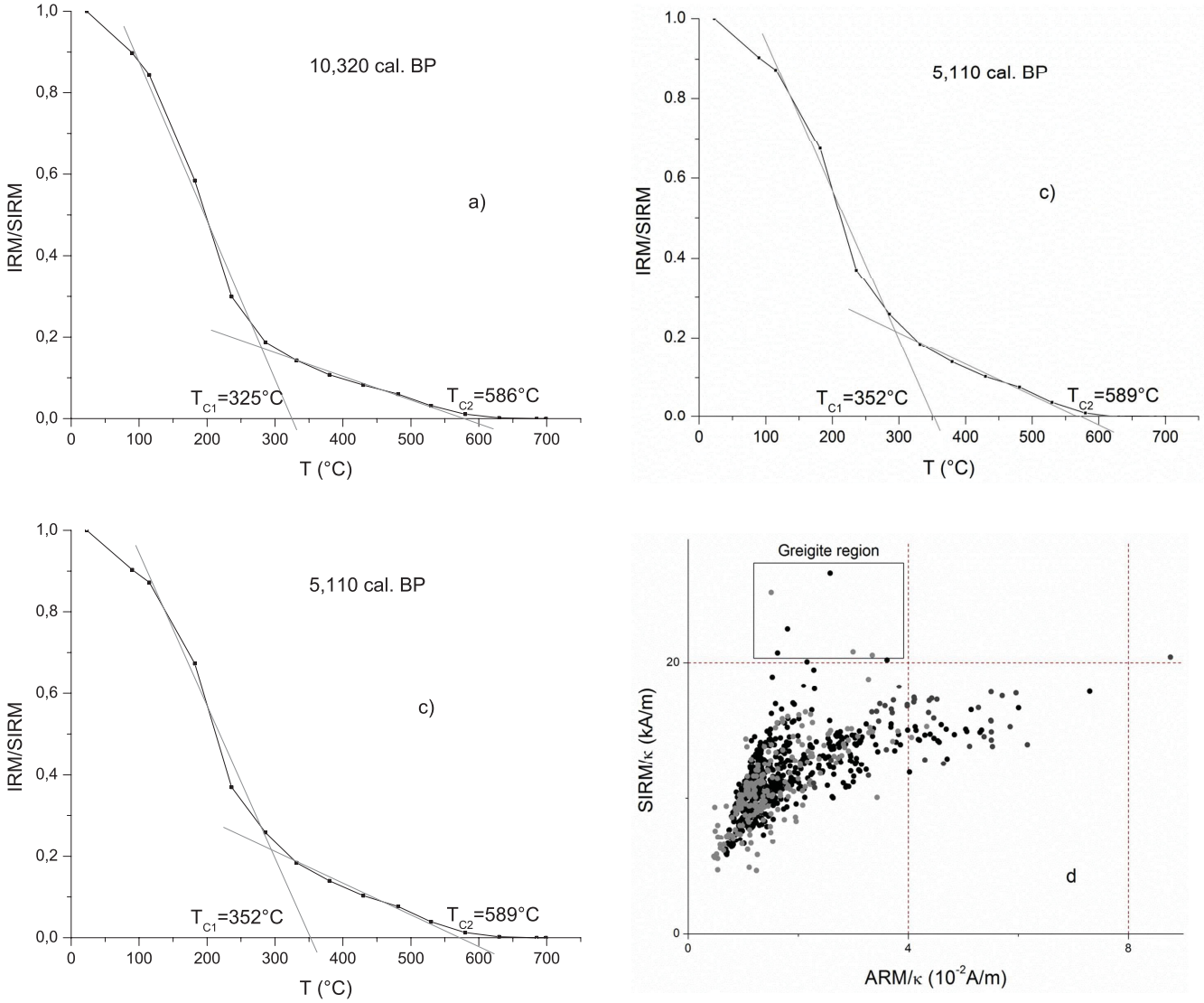

Figure 7. Greigite identification. Thermal demagnetization of the SIRM from room temperature to 700 °C for the sample located at (a) 10 320 cal. BP, (b) 8900 cal. BP and (c) 5110 cal. BP. (d) SIRM/k versus ARM/k, low values of ARM/k in samples with high SIRM/k are also indicators of the presence of greigite.

Frias (Ariztegui *et al.* 2008), Lago Argentino (Tonella *et al.* 2009) and Lago Fagnano (Waldmann *et al.* 2010), suggest the same trend.

8.2 Greigite and its palaeoclimatic considerations

Four samples with greigite as the main magnetic carrier were identified in the record at approximately 10 300, 8900, 8500 and 8300 cal. BP. To identify environmental scenarios that allow for the existence of greigite, it is necessary to investigate whether the greigite is authigenic or allochthonous. The samples were found in sectors of low Ti content at depths of 1403, 1225, 1115 and 1023 cm (Haberzettl *et al.* 2007), indicating that the allochthonous minerogenic input was low (Fig. 3c). Thus, greigite should have been formed within the lacustrine system. Additionally, Jouve *et al.* (2013) did not detect any micropumices (pyroclastic source) in the horizons where greigite was inferred according to the results presented in this study. For this reason, a detritic volcanic origin is ruled out for this mineral.

Considering an authigenic origin, greigite (ferrimagnetic) is an intermediate iron sulphide on the polysulphide pathway to pyrite (paramagnetic; Hunger & Benning 2007; Roberts *et al.* 2011). Although initially considered a rare mineral in sediments, greigite has become a common component in both lacustrine and marine anoxic sedimentary environments (e.g. Roberts & Turner 1993; Blanchet *et al.* 2009). Authigenic greigite is a mineral that is formed below the oxic-to-anoxic transition zone (OATZ). Below the OATZ, the degradation of organic matter involves a reaction with sulphates. This reaction can release sulphide ions that react with Fe^{2+} to form greigite (Fe_3S_4). A further source of this mineral is related to the action of sulphate-reducing bacteria that biosynthesise greigite (Falcon 2006). In addition, certain sedimentary conditions support the preservation of greigite by inhibiting its complete transformation into pyrite. These conditions are associated with rapid burial related to high sedimentation rates. Blanchet *et al.* (2009) observed greigite-bearing layers associated with flood deposits composed of terrigenous-rich and organic-poor sedimentary layers. These researchers propose that greigite preservation in those sediments was enabled by relative enrichment in organic matter over reactive iron and/or hydrogen sulphide. The generation of greigite is possible even under oligotrophic conditions when there is rapid sedimentation and stratification of lake water, as is the case in our record and in

the conditions proposed by Massaferro *et al.* (2013) and Zolitschka *et al.* (2013).

To form greigite in a lacustrine system, the lake water must be stratified and the sediment/water interface must be under reducing conditions (Evans & Heller 2003). Because of this consideration, the lake could have been stratified during at least four short periods. In these cases, lake stratification may be primarily caused by an increase in the lake level and/or low wind speeds, which prevent water mixture and/or unusual low winter temperatures. Additionally, the sulphate content in the environment further limits the formation of greigite.

If there is too little sulphate, greigite will not form, and if there is too much sulphate, pyrite can form (e.g. Heil *et al.* 2009). Thus, the sulphate content has implications with respect to lake-level phases, with the presence of greigite indicating an intermediate lake level due to sulphate abundance that is controlled by evaporative processes. The availability of sulphate in sediments of the studied section should be less than the availability obtained by Vuillemin *et al.* (2013) for an older section of the same lake. This finding could indicate an association between periods with light wind and subsequent water stratification and periods of evaporation that are higher than those related to the diagenesis of the studied section.

Zolitschka *et al.* (2013) proposed constantly high lake levels with a slight decrease (option 2, Fig. 8), which appears to be in agreement with the magnetic results. The decrease in wind speed and/or atmospheric temperature deserves special attention. Anderson *et al.* (2009) conclude that the westerlies were intensified but move south (towards the Drake Passage, around 900 km south of Laguna Potrok Aike) for YD. Lake stratification was suggested by Jouve *et al.* (2013) for the period between 13 600 and 11 100 cal. BP because of relatively weak westerlies. In this study, an analysis is performed using palaeoclimatological models to document the palaeocondition in which greigite was formed.

Earth's climate began to shift from cold glacial to warmer interglacial during the early Holocene. In this transitional period (Pleistocene/Holocene), temperatures suddenly returned to near-glacial conditions for a short time. The evidence indicates that there were two major cooling events in the NH: one called the YD (Alley 2000), which was registered between 12 900 and 11 600 cal. BP, and the other called the 8.2 ka event (Alley *et al.* 1997; Alley & Ágústsdóttir 2005; Kobashi *et al.* 2007), which was registered between 8400 and 8000 cal. BP and had an amplitude that was approximately half that of the YD. Separate geologic evidence indicates that both events were triggered by the collapse of the remanent of the Hudson Bay ice dome dam and the subsequent catastrophic final drainage of the glacial lakes Agassiz and Ojibway in the Hudson Bay. Therefore, deep-water formation in the northern Atlantic was shut down, allowing fresh water to pool on the ocean surface. Melt-water floods reduced the salinity and density of the surface water in the North Atlantic, causing a reduction in the ocean's thermohaline circulation, which caused a reduction in the Atlantic Meridional Overturning Circulation (Fig. 9, left-hand panel). Recently, Broecker *et al.* (2010) investigated the YD and Ellison *et al.* (2006) investigated the 8.2 ka event, with both investigations adding new details to the previously hypothesised causes of the events and converging upon a consistent picture for both events.

The impact produced in the atmospheric-oceanic system is clearly observable in palaeoclimatic records from many parts of the world. The spatiotemporal variability of temperature and humidity/precipitation was very high. In the NH, a cooling was generalized for both the YD (Lowell & Kelly 2008) and the 8.2 ka event (Wanner *et al.* 2011). However, the signal of temperature

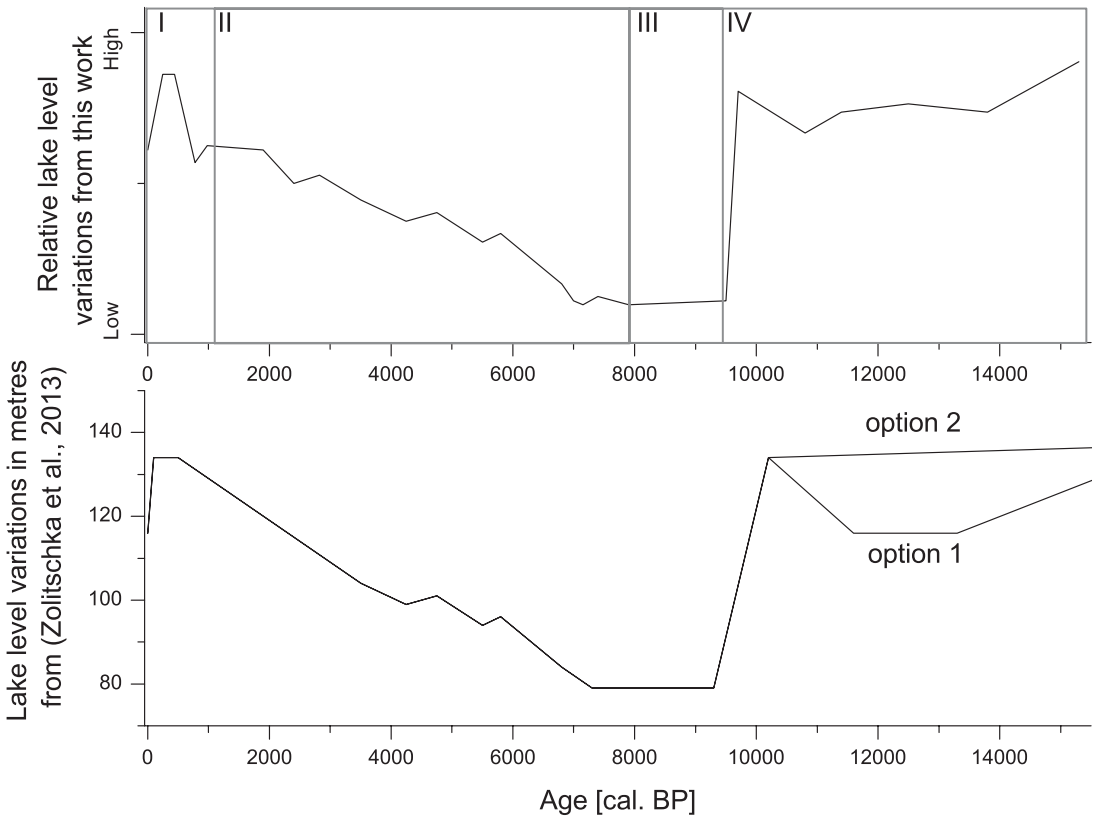

Figure 8. Lake-level variations reconstructed with rock magnetic data compared with published lake-level variations (Zolitschka *et al.* 2013).

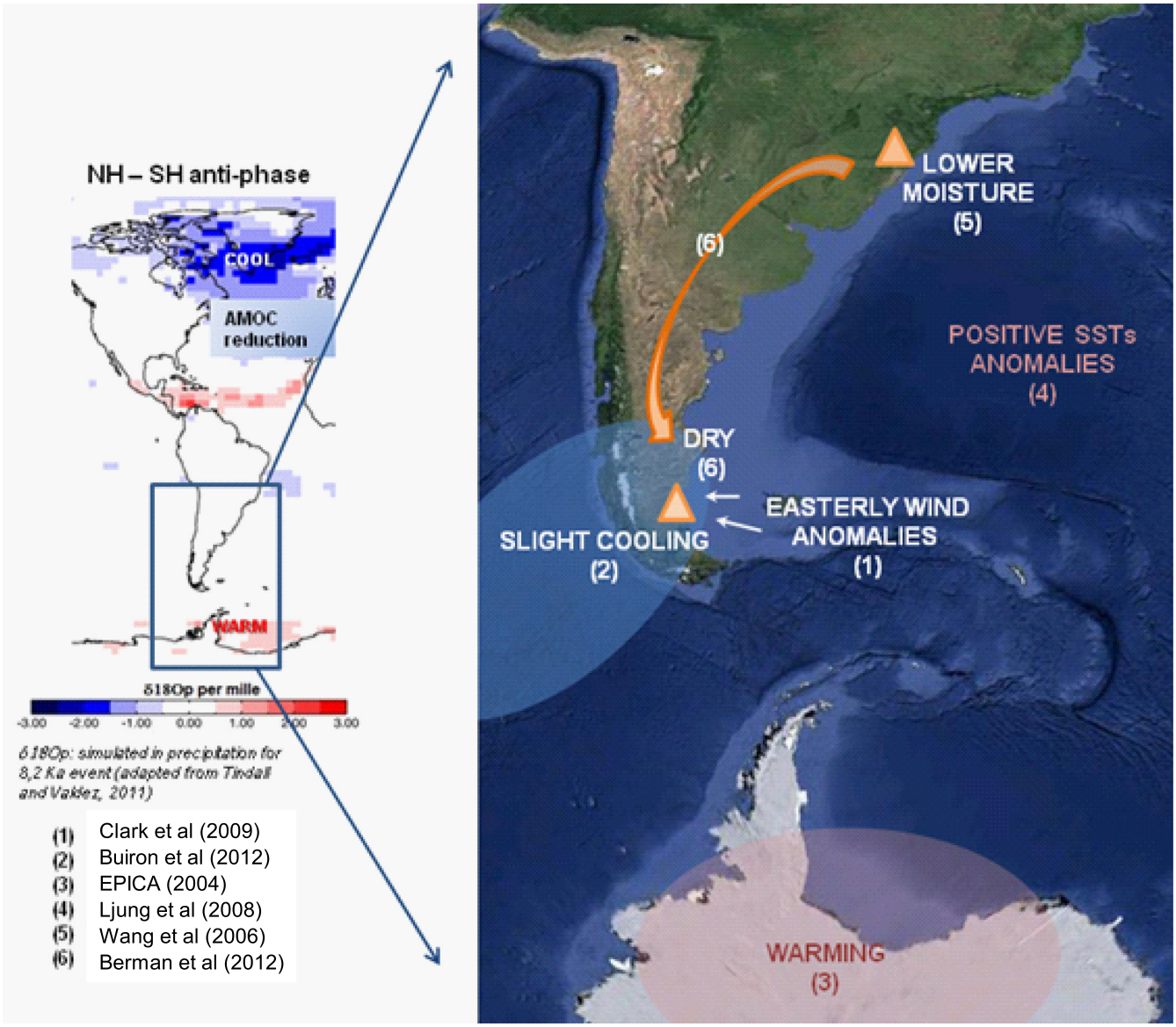

Figure 9. Schematic diagram showing the Northern Hemisphere–Southern Hemisphere links during the 8.2 Ka event (left) and climatic factors that affected the Potrok Aike area (right).

in the SH is currently under debate. In the case of the YD, advances of SH glaciers were registered prior to [during the Antarctic Cold Reversal (ACR)] or at the beginning of the event (Strelin & Malagnino 2000; Lowell & Kelly 2008). Furthermore, local glacial advances in the southern mid-latitudes were attributed to changes in southern-westerly wind circulation in the early Holocene rather than to YD-related cooling (Barrows *et al.* 2007). The ice core record at Dome C indicates that climate changes in Antarctica were out of phase with those in the NH, with a cooling (ACR) period prior to the YD followed by a warming period during the YD (EPICA 2004; Fig. 9). According to our record, no samples with greigite were found during the YD, suggesting mild temperatures consistent with other proxies from Laguna Potrok Aike. Greigite was found slightly after 11 600 cal. BP, suggesting a possible cooling. This finding is a delay with respect to the record of the YD in the NH.

For the 8.2 ka event, the empirical results also indicate a generalized cooling in the NH (Alley *et al.* 1997). Palaeoclimatic records from other parts of the world are rare, which makes it difficult to draw solid conclusions. Temperatures may have become warmer in Antarctica (EPICA 2004; Fig. 9). In addition, a lake sediment record from Nightingale Island in the central South Atlantic exhibits enhanced precipitation between 8275 and 8025 cal. BP, which was most likely due to increased sea-surface temperatures (Ljung *et al.* 2008; Fig. 9). Several concurrent records from the SH indicate cooler conditions at 8200 cal. BP (Morrill *et al.* 2012). Thus, temperature change in the SH appears to have been regionally heterogeneous. Additionally, Lal *et al.* (2007) presented a full characterization of the unique global 8.2 ka cooling event. Significant atmospheric cooling occurred from 9500 to 8500 cal. BP during three periods of approximately 50–100 yr when the sun was extremely quiet. Concurrent increases or decreases in the atmospheric $\Delta^{14}C$ levels occurred at 8500, 8200 and 8060 cal. BP. The low activity of the sun added to the flood of melt water into the North Atlantic from glacial lakes during the final demise of the Laurentide ice sheet.

Climatic model scenarios for the catastrophic 8.2 ka drainage of fresh water into the North Atlantic provide a wide range of results for the SH anomalies. However, all of the scenarios indicate a major cooling near the Labrador Sea and the North Atlantic together with a decrease in cooling towards the Equator. In the region under study, the simulated temperature anomaly results in a difference of between 0 and −1 °C with respect to the previous situation (Clarke *et al.* 2009), whereas other authors, such as LeGrande & Schmidt (2008) and Tindall & Valdes (2011), have obtained negligible anomalies in the region. Furthermore, Clarke *et al.* (2009) show scenarios with easterly wind anomalies that involve a weakening of the westerlies and/or a higher frequency of daily situations with E winds compared with previous conditions (Fig. 9).

Based on this finding, it is possible to speculate that the formation of greigite in the periods mentioned above was the product of seasonal stratification of the lake in periods with less oxygen in the hypolimnion. This stratification could have been caused by the weakening of the Westerlies and a slight cooling of the average temperature, as indicated by Buiron *et al.* (2012) and previously mentioned models (Fig. 9).

Several pulses of greigite genesis are observed in the sediment record and are in agreement with suggestions that the outbreak from Lake Agassiz occurred in two stages (Ellison *et al.* 2006; Dominguez-Villar *et al.* 2009): an earlier release at approximately 8490 cal. BP and a later release at approximately 8290 cal. BP. The 8.2 ka event occurred closer to the timing of the smaller release, suggesting a possible non-linear response to freshwater forcing. The suppositions about the formation of greigite are supported by the fact that greigite is also present close to the YD.

According to Wang *et al.* (2006), the 8.2 ka event in southern Brazil presented lower moisture than at present (Fig. 9). During summer and spring, this region is in phase with the modern environment in southern Patagonia (Berman *et al.* 2012; Fig. 9), which is consistent with the increasing particle size related to the gradual lowering of the lake level for the studied region of Patagonia. The pattern of precipitation variability indicates that the Laguna Potrok Aike region corresponds to the regime of southern Patagonia, whereas Lago Cardiel corresponds to the central region and a different regime (Berman *et al.* 2012). Based on this finding, there is a lack of correlation between the two lakes that is linked to humidity.

9 CONCLUSIONS

This study extends back 15 500 yr and allows inferences about lake-level changes by using a simple model based on magnetic parameters. If the lake sediment is dominated by allochtonous material and under consideration of a similar magnetic mineralogy, in-phase variations of magnetic concentration and grain size indicate lake-level fluctuations. High and low values for both parameters were interpreted as high and low lake levels, respectively. High lake levels were inferred in the intervals 15 300–13 800, 7400–7150 and 1100–860 cal. BP and from 700 cal. BP to the present, likely during 10 800–9700 cal. BP. Dry environments with low lake levels were observed in the intervals of 13 800–10 800 and 9 700–7400 cal. BP. A steady rise in the lake level was observed from 7000 to 1100 cal. BP. A good agreement between the applied model and several records from the lake was obtained, particularly between 10 000 cal. BP and the present.

Accordingly, the lake water column of Laguna Potrok Aike was stratified at least four times during the period studied, likely due to a weakening of the Westerlies and a slight regional cooling. The first stratification was at approximately 10 300 cal. BP, occurring slightly after the YD. The other three stratifications occurred at approximately 8900, 8500 and 8300 cal. BP and are related to the 8.2 ka event.

ACKNOWLEDGEMENTS

The authors wish to thank Universidad Nacional del Centro de la Provincia de Buenos Aires, Consejo Nacional de Investigaciones Científicas y Técnicas de la República Argentina (CONICET) as well as all of the SALSA and PASADO research-team members for their help with the fieldwork and their input during the discussions. This study is a contribution to the German Climate Research Program DEKLIM (01 LD 0034 and 0035), where funds were obtained for the 'South Argentinean Lake Sediment Archives and modelling' (SALSA) project. The authors would like to thank all of the funding agencies for their financial support, particularly UBA: UBACYT Nº:20020100101049, CONICET: PIP 747/10, PIP 114-201001-00250, PID-UTN1351, ARC/11/09 MINCYT (Argentina)-MEYS (Czech Republic). CG would like to thank the team of Geomorphologie und Polarforschung (GEOPOLAR) at the University of Bremen (Germany) for the kind assistance she received during her stay in Bremen. The subsampling work of CG was supported by the German Federal Ministry of Education and Research in the framework of the project 'Internationale Zusammenarbeit in Bildung und Forschung mit Argentinien Projekt ARG 08/A03', a scholarship of the LAC-ACCESS Programme 'Connecting high-quality research between the European Union and Latin American and Caribbean Countries' and the funding of Universidad Nacional del Centro (UNCPBA) through the Programme Línea B of SECAT-UNCPBA. The authors also wish to thank Google Earth for the satellite image of Fig. 9.

REFERENCES

Alley, R.B., 2000. The Younger Dryas cold interval as viewed from central Greenland, *Quatern. Sci. Rev.,* **19,** 213–226.

Alley, R.B. & Ágústsdóttir, A.M., 2005. The 8k event: cause and consequences of a major Holocene abrupt climate change, *Quatern. Sci. Rev.,* **24**(10–11), 1123–1149.

Alley, R.B., Mayewski, P.A., Sowers, T., Stuiver, M., Taylor, K.C. & Clark, P.U., 1997. Holocene climatic instability: a prominent, widespread event 8200 yr ago, *Geology,* **25,** 483–486.

Anderson, N.J. & Rippey, B., 1988. Diagenesis of magnetic minerals in the recent sediments of aeutrophic lake, *Limnol. Oceanogr.,* **33**(6, part 2), 1476–1492.

Anderson, R.F., Ali, S., Bradtmiller, L.I., Nielsen, S.H.H., Fleisher, M.Q., Anderson, B.E. & Burckle, L.H., 2009. Wind-driven upwelling in the southern ocean and the deglacial rise in atmospheric CO_2, *Science,* **323,** 1443–1448.

Anselmetti, F.S., Ariztegui, D., De Batist, M., Gebhardt, C., Haberzettl, T., Niessen, F., Ohlendorf, C. & Zolitschka, B., 2009. Environmental history of southern Patagonia unravelled by the seismic stratigraphy of Laguna Potrok Aike, *Sedimentology,* **56,** 873–892.

Ariztegui, D. & Dobson, J., 1996. Magnetic investigations of framboidal greigite formation: a record of anthropogenic environmental changes in eutrophic Lake St Moritz, Switzerland, *Holocene,* **6**(2), 235–241.

Ariztegui, D., Anselmetti, F.S., Gilli, A. & Waldmann, N., 2008. Late Pleistocene environmental change in eastern Patagonia and Tierra del Fuego—a limnnogeological approach, in *The Late Cenozoic of Patagonia and Tierra del Fuego,* pp. 241–253, ed. Rabassa, J., Elsevier.

Barrows, T.T., Lehman, S.J., Fifield, L.K. & De Deckker, P., 2007. Absence of cooling in New Zealand and the adjacent ocean during the Younger Dryas chronozone, *Science,* **318,** 86–89.

Berman, A.L., Silvestri, G. & Compagnucci, R., 2012. On the variability of seasonal temperature in southern South America, *Clim. Dynam.,* **40**(7–8), 1863–1878.

Blanchet, C.L., Thouveny, N., Vidal, L., Leduc, G., Tachikawa, K., Bard, E. & Beaufort, L., 2007. Terrigenous input response to glacial/interglacial climatic variations over southern Baja California: a rock magnetic approach, *Quatern. Sci. Rev.,* **26,** 3118–3133.

Blanchet, C.L., Thouveny, N. & Vidal, L., 2009. Formation and preservation of greigite (Fe3S4) in sediments from the Santa Barbara Basin: implications for paleoenvironmental changes during the past 35 ka, *Paleoceanography,* **24,** PA2224, doi:0.1029/2008PA001719.

Bradley, R.S., 1999. *Paleoclimatology,* 614 p. Elsevier.

Broecker, W.S., Denton, G H., Lawrence Edwards, R., Cheng, H., Alley, R.B. & Putnam, A.E., 2010. Putting the Younger Dryas cold event into context, *Quatern. Sci. Rev.,* **29,** 1078–1081.

Brown, L.C. & Duguay, C.R., 2010. The response and role of ice cover in lake-climate interactions, *Prog. Phys. Geogr.,* **34**(5), 671–704.

Buiron, D. *et al.*, 2012. Regional imprints of millennial variability during the MIS 3 period around Antarctica, *Quatern. Sci. Rev.,* **48,** 99–112.

Cartwright, A., Quade, J., Stine, S., Adams, K.D., Broecker, W. & Cheng, H., 2011. Chronostratigraphy and lake-level changes of Laguna Cari-Laufquén, Río Negro, Argentina, *Quatern. Res.,* **76,** 430–440.

Clarke, G.K., Bush, A.B.G. & Bush, J.W.M., 2009. Freshwater discharge, sediment transport, and modeled climate impacts of the final drainage of Glacial Lake Agassiz, *J. Clim.,* **22,** 2161–2180.

Coronato, A., Ercolano, B., Corbella, H. & Tiberi, P., 2013. Glacial, fluvial and volcanic landscape evolution in the Laguna Potrok Aike maar area, southernmost Patagonia, Argentina, *Quatern. Sci. Rev.,* **71,** 13–26.

Dankers, P.H., 1978. *Magnetic Properties of Dispersed Natural Iron Oxides of Known Grain Size,* 3rd edn, Univ. Utrecht.

Dearing, J.A., Hu, Y., Doody, P., James, P.A. & Brauer, A., 2001. Preliminary reconstruction of sediment-source linkages for the past 6000 yrs at the Petit Lac d´Annecy, France, based on mineral magnetic data, *J. Paleolimnol.,* **25,** 245–258.

Dekkers, M.J., Passier, H.F. & Schoonen, M.A.A., 2000. Magnetic properties of hydrothermally synthesized greigite (Fe3S4)—II. High- and low-temperature characteristics, *Geophys. J. Int.,* **141,** 809–819.

Demory, F., Oberhnsli, H., Nowaczyk, N.R., Gottschalk, M., Wirth, R. & Naumann, R., 2005. Detrital input and early diagenesis in sediments from Lake Baikal revealed by rock magnetism, *Global Planet. Change,* **46,** 145–166.

Dominguez-Villar, D., Fairchild, I.J., Baker, A., Wang, X., Edwards, R.L. & Cheng, H., 2009. Oxygen isotope precipitation anomaly in the North Atlantic region during the 8.2 ka event, *Geology,* **37,** 1095–1098.

Dunlop, D.J., 2002. Theory and application of the Day plot (M_{rs}/M_s versus H_{cr}/H_c) 1. Theoretical curves and tests using titanomagnetite data, *J. geophys. Res.,* **107,** B32056, doi:10.1029/2001JB000486.

Dunlop, D.J. & Özdemir, Ö., 1997. *Rock Magnetism. Fundamentals and Frontiers,* 573 pp, Cambridge Univ. Press.

Ellison, C.R.W., Chapman, M.R. & Hall, I.R., 2006. Surface and deep ocean interactions during the cold climate event 8200 years ago, *Science,* **312,** 1929–1932.

Endlicher, W., 1993. Klimatische Aspekte der Weidedegradation in Ost-Patagonien, in *BeiträgezurKultur- und Regionalgeographie. Festschrift für Ralph Jätzold,* pp. 91–103, eds. Hornetz, B. & Zimmer, D., Geographische GesellschaftTrier.

EPICA community members, 2004. Eight glacial cycles from an Antarctic ice core, *Nature,* **429,** 623–628.

Evans, M. & Heller, F., 2003. *Environmental Magnetism. Principles and Applications of Enviromagnetics,* 317 pp. Academic Press, Elsevier.

Falcon, K.J.M., 2006. Influenciaclimática, diagenética y antropogénica sobre la señal magnética y geoquímica de los sedimentos marinos cuaternarios del noroeste de la Península Ibérica, *PhD thesis,* Universidad de Vigo, España, 298 pp.

Frank, U., Nowaczyk, N.R., Negendank, J.F.W. & Melles, M., 2002. A paleomagnetic record from Lake Lama, northern Central Siberia, *Phys. Earth planet. Inter.,* **133,** 3–20.

Geiss, C.E., Umbanhowar, Ch.E., Camill, P. & Banerjee, S.K., 2003. Sediment magnetic properties reveal Holocene climate change along the Minnesota prairie-forest ecotone, *J. Paleolimnol.,* **30,** 151–166.

Gogorza, C.S.G., Sinito, A.M., Ohlendorf, C., Kastner, S. & Zolitschka, B., 2011. Paleosecular variation and paleointensity records for the last millennium from southern South America (Laguna Potrok Aike, Santa Cruz, Argentina), *Phys. Earth planet. Inter.,* **184,** 41–50.

Gogorza, C.S.G. *et al.*, 2012. High-resolution paleomagnetic records from Laguna PotrokAike (Patagonia, Argentina) for the last 16,000 years, *Geochem. Geophys. Geosystems,* **13,** Q12Z37, doi:10.1029/2011GC003900.

Haberzettl, T. *et al.*, 2005. Climatically induced lake level changes during the last two millennia as reflected in sediments of Laguna Potrok Aike, southern Patagonia (Santa Cruz, Argentina), *J. Paleolimnol.,* **33,** 283–302.

Haberzettl, T. *et al.*, 2007. Late glacial and Holocene wet-dry cycles in southern Patagonia: chronology, sedimentology and geochemistry of a lacustrine record from Laguna Potrok Aike, Argentina, *Holocene,* **17,** 297–310.

Hahn, A., Kliem, P., Ohlendorf, C., Zolitschka, B. & Rosén, P. the PASADO Science Team, 2013. Climate induced changes as registered in inorganic and organic sediment components from Laguna Potrok Aike (Argentina) during the past 51 ka, *Quatern. Sci. Rev.,* **71,** 154–166.

Heil, C.W., King, J.W., Rosenbaum, J.G., Reynolds, R.L. & Colman, S.M., 2009. Paleomagnetism and environmental magnetism of GLAD800 sediment cores from Bear Lake, Utah and Idaho, *Geol. Soc. Am. Special Papers,* **450,** 291–310.

Hilgenfeldt, K., 2000. Diagenetic dissolution of biogenic magnetite in surface sediments of the benguela upwelling system, *Int. J. Earth Sci.,* **88,** 630–640.

Hu, S., Appel, E., Hoffmann, V. & Schmahl, W., 2002. Identification of greigite in lake sediments and its magnetic significance, *Sci. China Series D: Earth Sci.,* **45,** 81–87.

Hunger, S. & Benning, L.G., 2007. Greigite: a true intermediate on the polysulfide pathway to pyrite, *Geochem. Trans.,* **8,** 1, doi:10.1186/1467-4866-8-1.

Irurzun, M.A., Gogorza, C.S.G., Torcida, S., Lirio, J.M., Nuñez, H., Bercoff, P.G., Chaparro, M.A.E. & Sinito, A.M., 2009. Rock magnetic properties and relative paleointensity stack between 13 and 24 kyr BP calibrated ages from sediment cores, Lake Moreno (Patagonia, Argentina), *Phys. Earth planet. Inter.,* **172,** 157–168.

Jouve, G., Francus, P., Lamoureux, S., Provencher-Nolet, L., Hahn, A., Haberzettl, T., Fortin, D. & Nuttin, L. the PASADO Science Team, 2013. Microsedimentological characterization using image analysis and m-XRF as indicators of sedimentary processes and climate changes during Lateglacial at Laguna Potrok Aike, Santa Cruz, Argentina, *Quatern. Sci. Rev.,* **71,** 191–204.

Kelts, K., Briegel, U., Ghilardi, K. & Hsü, K., 1986. The limnogeology-ETH coring system Schweiz, *Z. Hydrol.,* **48,** 104–115.

Kilian, R., Hohner, M., Biester, H., Wallrabe-Adams, H.J. & Stern, C.R., 2003. Holocene peat and lake sediment tephra record from the southernmost Chilean Andes (53°–55°S), *RevistaGeológica de Chile,* **30,** 23–37.

Kliem, P. *et al.*, 2013a. Magnitude, geomorphologic response and climate links of lake level oscillations at Laguna PotrokAike, Patagonian steppe (Argentina), *Quatern. Sci. Rev.,* **71,** 131–146.

Kliem, P. *et al.*, 2013b. Lithology, radiocarbon chronology and sedimentological interpretation of the lacustrine record from Laguna Potrok Aike, southern Patagonia, *Quatern. Sci. Rev.,* **71,** 54–69.

Kobashi, T, Severinghaus, J.P., Brook, E.J., Barnola, J.M. & Grachev, A.M., 2007. Precise timing and characterization of abrupt climate change 8200 years ago from air trapped in polar ice, *Quatern. Sci. Rev.,* **26,** 1212–1222.

Lal, D., Largem, W.G. & Walker, S.G., 2007. Climatic forcing before, during, and after the 8.2 kyr BP global cooling event, *J. Earth Sys. Sci.,* **116,** 171–177.

Lanci, L., Hirt, A.M., Lowriea, W., Lotter, A.F., Lemcke, G. & Sturm, M., 1999. Mineral-magnetic record of Late Quaternary climatic changes in a high Alpine lake, *Earth planet. Sci. Lett.,* **170**(1–2), 49–59.

LeGrande, A.N. & Schmidt, G.A., 2008. Ensemble, water isotope-enabled, coupled general circulation modeling insights into the 8.2 ka event, *Paleoceanography,* **23,** PA3207, doi:10.1029/2008PA001610.

Lisé-Pronovost, A., St-Onge, G., Gogorza, C., Haberzettl, T., Preda, M., Kliem, P., Francus, P. & Zolitschka, B. the PASADO Science Team, 2013. High-resolution paleomagnetic secular variations and relative paleointensity since the Late Pleistocene in southern South America, *Quatern. Sci. Rev.,* **71,** 91–108.

Ljung, K., Björck, S., Renssen, H. & Hammarlund, D., 2008. South Atlantic island record reveals a South Atlantic response to the 8.2 kyr event, *Clim. Past,* **4,** 35–45.

Lowell, T.V. & Kelly, M.A., 2008. Was the younger dryas global? *Science,* **231,** 348–349.

Mancini, M.V., Paez, M.M., Prieto, A.R., Stutz, S., Tonello, M. & Vilanova, I., 2005. Mid-Holocene climatic variability reconstruction from pollen records (32°–52°S, Argentina), *Quatern. Int.,* **132,** 47–59.

Markgraf, V., 1983. Late and postglacial vegetational and palaeoclimatic changes in Subantarctic, temperate, and arid environments in Argentina, *Palynology,* **7,** 43–70.

Massaferro, J., Recasens, C., Larocque-Tobler, I., Maidana, N.I. & Zolitschka, B., 2013. Major lake level fluctuations and climate changes for the past 16,000 years as reflected by diatoms and chironomids preserved in the sediment of Laguna Potrok Aike, southern Patagonia, *Quatern. Sci. Rev.,* **71,** 167–174.

Mayr, C. *et al.*, 2009. Isotopic fingerprints on lacustrine organic matter from Laguna Potrok Aike (southern Patagonia, Argentina) reflect environmental changes during the last 16,000 years, *J. Paleolimnol.,* **42,** 81–102.

Mayr, C. *et al.*, 2013. Intensified Southern Hemisphere Westerlies regulated atmospheric CO_2 during the last deglaciation, *Geology,* **41**(8), 831–834.

Morrill, C., Anderson, D.M., Bauer, B.A., Buckner, R., Gille, E.P., Gross, W.S., Hartman, M. & Shah, A., 2012. Proxy benchmarks for intercomparison of 8.2 ka simulations, *Clim. Past Discuss.,* **8,** 3765–3789.

Nichols, G., 2009. *Sedimentology and Stratigraphy,* 2nd edn, Wiley, 419 pp.

Ohlendorf, C. *et al.*, 2013. Mechanisms of lake-level change at Laguna Potrok Aike (Argentina) e insights from hydrological balance calculations, *Quatern. Sci. Rev.,* **71,** 27–45.

Oliva, G., González, L., Rial, P. & Livraghi, E., 2001. El ambiente en la Patagonia Austral, in *Ganadería Ovina Sustentable en la Patagonia Austral,* pp. 19–82, eds. Borrelli, P. & Oliva, G., INTA Centro Regional Patagonia Sur.

Orgeira, M.J., Walther, A.M., Tófalo, R.O., Vásquez, C., Berquó, T., Favier Dobois, C. & Bohnel, H., 2003. Environmental magnetism in fluvial and loessic Holocene sediments and paleosols from the Chacopampean plain (Argentina), *J. S. Am. Earth Sci.,* **16,** 259–274.

Paasche, Ø., Løvlie, R., Dahl, S.O., Bakke, J. & Nesje, A., 2004. Bacterial magnetite in lake sediments: late glacial to Holocene climate and sedimentary changes in northern Norway, *Earth planet. Sci. Lett.,* **223,** 319–333.

Peck, J.A., Green, R.R., Shanahan, T., King, J.W., Overpeck, J.T. & Scholz, C.A., 2004. A magnetic mineral record of Late Quaternary tropical climate variability from Lake Bosumtwi, Ghana, *Palaeogeog. Palaeclimat. Palaeoecol.,* **215,** 37–57.

Peters, C. & Dekkers, M.J., 2003. Selected room temperature magnetic parameters as a function of mineralogy, concentration and grain size, *Phys. Chem. Earth,* **28,** 659–667.

Richter, C., Venuti, A., Verosub, K.L. & Wei, K.-Y., 2006. Variations of the geomagnetic field during the Holocene: relative paleointensity and inclination record from the West Pacific (ODP Hole 1202B), *Phys. Earth planet. Inter.,* **156,** 179–193.

Roberts, A. & Turner, G., 1993. Diagenetic formation of ferromagnetic iron sulphide minerals in rapidly deposited marine sediments, New Zealand, *Earth planet. Sci. Lett.,* **115,** 257–273.

Roberts, A.P., Chang, L., Rowan, C.J., Horng, C.S. & Florindo, F., 2011. Magnetic properties of sedimentary greigite (Fe3S4): an update, *Rev. Geophys.,* **49,** RG1002, doi:10.1029/2010RG000336.

Rühland, K., St. Jacques, J.M., Beierle, B.D., Lamoureux, S.F., Dyke, A.S. & Smol, J.P., 2009. Lateglacial and Holocene paleoenvironmental changes recorded in lake sediments, Brock Plateau (Melville Hills), Northwest Territories, Canada, *Holocene,* **19**(7), 1005–1016.

Schäbitz, F. *et al.*, 2013. Reconstruction of paleoprecipitation based on pollen transfer functions–the record of the last 16 ka from Laguna Potrok Aike, southern Patagonia, *Quatern. Sci. Rev.,* **71,** 175–190.

Stockhausen, H. & Zolitschka, B., 1999. Environmental changes since 13,000 cal. BP reflected in magnetic and sedimentological properties of sediments from, Lake Holzmaar (Germany), *Quatern. Sci. Rev.,* **18,** 913–925.

Strelin, J.A. & Malagnino, E.C., 2000. Late-glacial history of Lago Argentino, Argentina, and age of the Puerto Bandera Moraines, *Quat. Res,* **54,** 339–347.

Tauxe, L., Mullender, T. & Pick, T., 1996. Potbellies, wast-waists, and superparamagnetism in magnetic hysteresis, *J. geophys. Res.,* **101**(B1), 571–583.

Thompson, R. & Oldfield, F., 1986. *Environmental Magnetism,* 227 pp. Allen and Unwin Ltd.

Tindall, J. & Valdes, P.J., 2011. Modeling the 8.2 ka event using a coupled atmosphere–ocean GCM, *Global Planet. Change,* **79,** 312–321.

Tonella, M.S., Mancini, M.V. & Seppä, H., 2009. Quantitative reconstruction of Holocene precipitation changes in southern Patagonia, *Quatern. Res.,* **72,** 410–420.

Turner, G.M., 1997. Environmental magnetism and magnetic correlation of high resolution lake sediment records from Northern Hawke´s Bay, New Zealand, *J. Geol. Geophys.,* **40,** 287–298.

Vázquez, G., 2012. Magnetismo Ambiental de los Últimos 17,000 años en el Lago Zirahuén, Michoacán, México, *PhD thesis,* Universidad Nacional Autónoma de México, México.

Vázquez, G., Ortega, B., Davies, S.J. & Aston, B.J., 2010. Registro sedimentario de los últimos ca. 17000 años del lago de Zirahuén, Michoacán, México, *Boletín de la Sociedad Geológica Mexicana,* **62**(3), 325–343.

Vigliotti, L., Verosub, K.L., Cattaneo, A., Trincardi, F., Asioli, A. & Piva, A., 2008. Palaeomagnetic and rock magnetic analysis of Holocene deposits from the Adriatic Sea: detecting and dating short-term fluctuations in sediment supply, *Holocene,* **18,** 141–152.

Vuillemin, A., Ariztegui, D., De Coninck, A.S., Lücke, A., Mayr, C. & Schubert, C.J. the PASADO Scientific Team, 2013. Origin and significance of diagenetic concretions in sediments of Laguna Potrok Aike, southern Argentina, *J. Paleolimnol.,* **50**(3), 275–291.

Waldmann, N., Ariztegui, D., Anselmetti, F.S., Austin, J.A., Stern, C., Moy, C.M., Recasens, C. & Dunbar, R., 2010. Holocene climatic fluctuations and positioning of the Southern Hemisphere westerlies in Tierra del Fuego (54°S), Patagonia, *J. Quatern. Sci.,* **25**(7), 1063–1075.

Wang, X., Auler, A.S., Edwards, R.L., Cheng, H., Ito, E. & Solheid, M., 2006. Interhemispheric anti-phasing of rainfall during the last glacial period, *Quatern. Sci. Rev.,* **25,** 3391–3403.

Wanner, H., Solomina, O., Grosjean, M., Ritz, S.P. & Jetel, M., 2011. Structure and origin of Holocene cold events, *Quatern. Sci. Rev.,* **30,** 3109–3123.

Wille, M. *et al.*, 2007. Vegetation and climate dynamics in southern South America: the microfossil record of Laguna Potrok Aike, Santa Cruz, Argentina, *Rev. Palaeobot. Palynol.,* **146,** 234–246.

Zhu, J., Lücke, A., Wissel, H., Müller, D., Mayr, C., Ohlendorf, C. & Zolitschka, B. the PASADO Science Team, 2013. The last Glacial-Interglacial transition in Patagonia, Argentina: the stable isotope record of bulk sedimentary organic matter from Laguna Potrok Aike, *Quatern. Sci. Rev.,* **71,** 20–218.

Zolitschka, B. *et al.*, 2006. Crater lakes of the Pali Aike Volcanic Field as key sites for paleoclimatic and paleoecological reconstructions in southern Patagonia, Argentina, *J. S. Am. Earth Sci.,* **21,** 294–309.

Zolitschka, B. *et al.*, 2013. Environment and climate of the last 51,000 years e new insights from the PotrokAike maar lake Sediment Archive Drilling prOject (PASADO), *Quatern. Sci. Rev.,* **71,** 1–12.

SUPPORTING INFORMATION

Additional Supporting Information may be found in the online version of this article:

Figure S1. Hysteresis loop (black: uncorrected, grey: corrected) found in (a) 95 per cent of the samples, suggesting magnetite as main magnetic carrier (*cf.* Dunlop & Özdemir 1997) and (b) in 5 per cent of the samples suggesting hard magnetic minerals like greigite (*cf.* Roberts *et al.* 2011). (c) H_{CR}/H_C versus M_{RS}/M_S ratios indicating the relationship of hysteresis parameters (Dunlop 2002). MD: multi domain, SD: single domain, PSD: pseudo-single domain, SP: superparamagnetic.

Figure S2. Fig. 3 from Gogorza *et al.* (2012). Rock magnetic studies: (a) Thermal demagnetization results of the Saturation of the Isothermal Remanent Magnetization (SIRM) and (b) Normalized Isothermal Remanent Magnetization (IRM) acquisition curves, for representative samples from core PTA03/12. (c) Susceptibility (k) versus Saturation of the Isothermal Remanent Magnetization (SIRM) for all samples in order to estimate concentration and grain size, according to Thompson & Oldfield (1986). (d) Frequency dependence factor (F_{factor}) versus depth (http://gji.oxfordjournals.org/lookup/suppl/doi:10.1093/gji/ggu155/-/DC1).

Please note: Oxford University Press is not responsible for the content or functionality of any supporting materials supplied by the authors. Any queries (other than missing material) should be directed to the corresponding author for the article.